IOP Publishing Journal of Physics B: Atomic, Molecular and Optical Physics
J. Phys. B: At. Mol. Opt. Phys. **47** (2014) 195202 (6pp) doi:10.1088/0953-4075/47/19/195202

Neutron-impact ionization of He

M S Pindzola[1], T G Lee[1], Sh A Abdel-Naby[1], F Robicheaux[2], J Colgan[3] and M F Ciappina[4]

[1] Department of Physics, Auburn University, Auburn, AL, USA
[2] Department of Physics, Purdue University, West Lafayette, IN, USA
[3] Theoretical Division, Los Alamos National Laboratory, Los Alamos, NM, USA
[4] Max Planck Institute for Quantum Optics, Garching, Germany

E-mail: pindzms@auburn.edu

Received 5 June 2014, revised 11 August 2014
Accepted for publication 20 August 2014
Published 24 September 2014

Abstract

The time-dependent close-coupling method is used to calculate neutron-impact single and double ionization cross sections of the He atom. We also present the ratio of double to single ionization for He as a guide to experimental checks of theory at low energies and experimental confirmation of the rapid rise of the ratio at high energies unique to neutron-impact ionization of atoms.

Keywords: neutron, ionization, helium

(Some figures may appear in colour only in the online journal)

1. Introduction

The double ionization of He by either photon impact or bare ion impact are simple examples of the quantal three-body Coulomb breakup problem. For example, the double photoionization of He near threshold produces two slow moving continuum electrons in the Coulomb field of an alpha particle, which is extremely difficult for perturbation theory to handle. On the other hand, various non-perturbative theoretical approaches, including R-matrix methods [1–5], the converged close-coupling method [6], the time-dependent close-coupling (TDCC) method [7], and the exterior complex scaling (ECS) method [8] have yielded double photoionization cross sections for He in good agreement with experiment [9].

Another simple example is found in neutron scattering from the nucleus of the He atom [10, 11]. Depending on the energy acquired by the target nucleus, the atomic electrons can either follow its movement and remain in bound states or be released to the continuum. When both electrons are released to the continuum, we again have to solve the three-body breakup problem. Recently a non-perturbative ECS method was used to calculate neutron-impact single and double ionization cross sections for He [12]. They found significant differences in the ratio of double to single ionization cross sections from those found in photon impact and bare ion impact processes. With almost two dozen neutron scattering facilities in the world [13], a better understanding of the motion of atomic electrons following neutron-impact could provide insight into many neutron research projects in not only physics, but astronomy, biology, chemistry, and engineering. For example, new detectors are currently being designed to search for weakly interacting massive particles (dark matter candidates) based on neutron scattering experiments [14].

In this paper we present a theoretical study of the single and double ionization of He over a broad energy range. The non-perturbative TDCC method allows us to incorporate the interaction of two continuum electrons in the presence of a positive ion field in an accurate manner. We present total cross sections for the single, single with excitation, and double ionization of He. We compare cross section ratios of double to single ionization with previous ECS results [12]. We also present energy and angle differential cross sections for the single and double ionization of He.

The rest of the paper is organized as follows. In section 2 we present the non-perturbative TDCC method for neutron-impact ionization of atoms. In section 3 we present total and differential cross sections for the neutron-impact single and double ionization of He. In section 4 we conclude with a brief summary and future plans. Unless otherwise stated, we will use atomic units.

2. Theory

2.1. Elastic neutron–nucleus scattering

The neutron-impact ionization cross sections for atoms involve elastic cross sections for neutron scattering from

Table 1. Neutron-alpha particle head-on elastic cross sections [15] (1.0 barn = 1.0 $\times 10^{-24}$ cm^2).

E_n (keV)	E_α (keV)	$\sigma_{n\alpha}$ (barns)
10.0	1.6	0.755
20.0	3.2	0.740
40.0	6.4	0.711
60.0	9.6	0.658
80.0	12.8	0.605
100.0	16.0	0.552
150.0	24.0	0.499
200.0	32.0	0.371

the target atom nucleus. We make use of tabulated values from the National Nuclear Data Center (NNDC) for head-on collisions [15], that is collisions where the angle between the neutron and the target atom nucleus after the collision is zero. Using the conservation of energy and momentum, the speed at which the target atom nucleus takes off is given by

$$v_t = 2m_n v_n/(m_n + m_t), \tag{1}$$

where v_n is the incident neutron speed, m_n is the neutron mass, and m_t is the target atom nucleus mass. Thus for He atoms, $v_\alpha = \frac{2}{5}v_n$ and $E_\alpha = \frac{4}{25}E_n$. Using the NNDC tables [15] and

$$\sigma_{n\alpha}(E_n) = 4\pi \frac{d\sigma_{n\alpha}(E_n, \theta = 0)}{d\theta}\ , \tag{2}$$

we present neutron-alpha particle head-on elastic cross sections in table 1.

2.2. Time-dependent close-coupling equations

For single and double ionization in neutron collisions with two-electron atoms and ions, we solve the time-dependent Schrödinger equation given by:

$$i\frac{\partial \Psi(\vec{r}_1, \vec{r}_2, t)}{\partial t} = H(\vec{r}_1, \vec{r}_2)\Psi(\vec{r}_1, \vec{r}_2, t), \tag{3}$$

where

$$H(\vec{r}_1, \vec{r}_2) = \sum_{i=1,2}\left(-\frac{1}{2}\nabla_i^2 - \frac{Z}{r_i}\right) + \frac{1}{|\vec{r}_1 - \vec{r}_2|}\ . \tag{4}$$

If we expand $\Psi(\vec{r}_1, \vec{r}_2, t)$ in coupled spherical harmonics,

$$\Psi(\vec{r}_1, \vec{r}_2, t) = \sum_{l_1,l_2}\frac{P^{LM}_{l_1l_2}(r_1, r_2, t)}{r_1 r_2} \times \sum_{m_1,m_2} C^{l_1l_2L}_{m_1m_2M} Y_{l_1m_1}(\theta_1, \phi_1) Y_{l_2m_2}(\theta_2, \phi_2)\ , \tag{5}$$

the resulting close-coupled equations for the $P^{LM}_{l_1l_2}(r_1, r_2, t)$ radial wavefunctions are given by [16]

$$i\frac{\partial P^{LM}_{l_1l_2}(r_1, r_2, t)}{\partial t} = \sum_{i=1,2}\left(T_{l_i}(r_i)\right)P^{LM}_{l_1l_2}(r_1, r_2, t) + \sum_{l_1', l_2'} V^{L}_{l_1l_2,\, l_1'l_2'}(r_1, r_2) P^{LM}_{l_1'l_2'}(r_1, r_2, t)\ , \tag{6}$$

where

$$T_{l_i}(r_i) = -\frac{1}{2}\frac{\partial^2}{\partial r_i^2} + \frac{l_i(l_i+1)}{2r_i^2} - \frac{Z}{r_i}\ . \tag{7}$$

The two-body interaction operator is given by

$$V^{L}_{l_1l_2,\, l_1'l_2'}(r_1, r_2) = (-1)^{L+l_2+l_2'}\sqrt{(2l_1+1)(2l_1'+1)(2l_2+1)(2l_2'+1)} \times \sum_\lambda \frac{(r_1, r_2)^\lambda_<}{(r_1, r_2)^{\lambda+1}_>}\begin{pmatrix} l_1 & \lambda & l_1' \\ 0 & 0 & 0\end{pmatrix}\begin{pmatrix} l_2 & \lambda & l_2' \\ 0 & 0 & 0\end{pmatrix} \times \begin{Bmatrix} L & l_2' & l_1' \\ \lambda & l_1 & l_2\end{Bmatrix}. \tag{8}$$

2.3. Initial conditions

Following the neutron collision with the target atom nucleus, the atomic electrons see a nucleus moving off with speed $\vec{v} = v\hat{z}$. For rapid removal of the target atom nucleus, we make use of the sudden approximation. Thus, in the frame of reference of the target electrons, the initial condition is given by

$$\Psi(\vec{r}_1, \vec{r}_2, t = 0) = e^{-iv(z_1+z_2)}\bar{\Psi}(\vec{r}_1, \vec{r}_2)\ , \tag{9}$$

where $v = v_t = \frac{2}{5}v_n$ for He atoms. In terms of the radial wavefunctions the initial condition is given by

$$P^{LM}_{l_1l_2}(r_1, r_2, t = 0) = \sum_{l_1', l_2'}\bar{P}^{L_0M_0}_{l_1'l_2'}(r_1, r_2) \times \left\langle (l_1, l_2)LM \left| e^{-iv(z_1+z_2)} \right| (l_1', l_2')L_0M_0 \right\rangle\ , \tag{10}$$

where the ground state radial wavefunctions, $\bar{P}^{L_0M_0}_{l_1'l_2'}(r_1, r_2)$, are obtained by relaxation of the close-coupled equations of equation (6) in imaginary time. The angular matrix elements for e^{-ivz_1} are given by

$$\left\langle (l_1, l_2)LM \left| e^{-ivz_1} \right| (l_1', l_2')L_0M_0 \right\rangle = (-1)^{L+L_0-M+l_2}\delta_{l_2,l_2'} \times \sqrt{(2L+1)(2L_0+1)(2l_1+1)(2l_1'+1)} \times \sum_\lambda (-i)^\lambda (-1)^\lambda (2\lambda+1) j_\lambda(vr_1) \times \begin{pmatrix} l_1 & \lambda & l_1' \\ 0 & 0 & 0\end{pmatrix}\begin{pmatrix} L & \lambda & L_0 \\ -M & 0 & M_0\end{pmatrix} \times \begin{Bmatrix} l_1 & l_2 & L \\ L_0 & \lambda & l_1'\end{Bmatrix}, \tag{11}$$

the angular matrix elements for e^{-ivz_2} are given by

$$\begin{aligned}\left\langle (l_1, l_2)LM \left| e^{-ivz_2} \right| (l_1', l_2')L_0M_0 \right\rangle &= (-1)^{M+l_1+l_2'+l_2}\delta_{l_1,l_1'} \\ &\times \sqrt{(2L+1)(2L_0+1)(2l_2+1)(2l_2'+1)} \\ &\times \sum_{\lambda} (-i)^{\lambda}(-1)^{\lambda}(2\lambda+1) j_{\lambda}(vr_2) \\ &\times \begin{pmatrix} l_2 & \lambda & l_2' \\ 0 & 0 & 0 \end{pmatrix} \begin{pmatrix} L & \lambda & L_0 \\ -M & 0 & M_0 \end{pmatrix} \\ &\times \begin{Bmatrix} l_1 & l_2 & L \\ \lambda & L_0 & l_2' \end{Bmatrix}, \end{aligned} \tag{12}$$

and $j_{\lambda}(vr)$ are spherical Bessel functions.

The reduction of the initial condition of equation (10) begins with the insertion of a complete set of states, $|(l_1'', l_2'')L''M''\rangle$, such that

$$\begin{aligned} P_{l_1l_2}^{LM}(r_1, r_2, t=0) &= \sum_{l_1', l_2'} \bar{P}_{l_1'l_2'}^{L_0M_0}(r_1, r_2) \\ &\times \sum_{l_1'', l_2''} \sum_{L'', M''} \left\langle (l_1, l_2)LM \left| e^{-ivz_1} \right| (l_1'', l_2'')L''M'' \right\rangle \\ &\times \left\langle (l_1'', l_2'')L''M'' \left| e^{-ivz_2} \right| (l_1', l_2')L_0M_0 \right\rangle. \end{aligned} \tag{13}$$

Using the fact that $L_0 = M_0 = 0$ for the ground state and equations (11)–(12) for the coupled state matrix elements, the initial condition can be expressed as

$$\begin{aligned} P_{l_1l_2}^{L0}(r_1, r_2, t=0) &= (-1)^{L}\sqrt{(2L+1)(2l_1+1)(2l_2+1)} \\ &\times \sum_{l_1', l_2'} \bar{P}_{l_1'l_2'}^{00}(r_1, r_2)(-1)^{l_1'+l_2'}\sqrt{(2l_1'+1)(2l_2'+1)} \\ &\times \sum_{\lambda, \lambda'} (-i)^{\lambda+\lambda'}(-1)^{\lambda}(2\lambda+1)(2\lambda'+1)^2 j_{\lambda}(vr_1) j_{\lambda'}(vr_2) \\ &\times \begin{pmatrix} l_1 & \lambda & l_1' \\ 0 & 0 & 0 \end{pmatrix} \begin{pmatrix} L & \lambda & \lambda' \\ 0 & 0 & 0 \end{pmatrix} \\ &\times \begin{pmatrix} l_2 & \lambda' & l_2' \\ 0 & 0 & 0 \end{pmatrix} \begin{pmatrix} \lambda' & \lambda' & 0 \\ 0 & 0 & 0 \end{pmatrix} \\ &\times \begin{Bmatrix} l_1 & l_2 & L \\ \lambda' & \lambda & l_1' \end{Bmatrix} \begin{Bmatrix} l_1' & l_2 & \lambda' \\ \lambda' & 0 & l_2' \end{Bmatrix}. \end{aligned} \tag{14}$$

We note that the interaction of the neutron with the atomic electrons takes place completely through the initial condition of equation (14).

2.4. Scattering probabilities and cross sections

Following the time propagation of equation (6) with the initial conditions of equation (14), single ionization probability amplitudes are given by

$$\mathscr{P}_{+}^{L}(n_1l_1, k_2l_2) = \int_0^{\infty} dr_1 \int_0^{\infty} dr_2 P_{n_1l_1}(r_1) P_{k_2l_2}(r_2) \hat{P}_{l_1l_2}^{L0}(r_1, r_2, t \to \infty), \tag{15}$$

and double ionization probability amplitudes are given by

$$\mathscr{P}_{++}^{L}(k_1l_1, k_2l_2) = \int_0^{\infty} dr_1 \int_0^{\infty} dr_2 P_{k_1l_1}(r_1) P_{k_2l_2}(r_2) \hat{P}_{l_1l_2}^{L0}(r_1, r_2, t \to \infty), \tag{16}$$

where

$$\begin{aligned} \hat{P}_{l_1l_2}^{L0}(r_1, r_2, t \to \infty) &= P_{l_1l_2}^{L0}(r_1, r_2, t \to \infty) \\ &- \beta \bar{P}_{ll}^{00}(r_1, r_2)\delta_{L,0}\delta_{l_1,l}\delta_{l_2,l} \end{aligned} \tag{17}$$

and

$$\begin{aligned} \beta = \sum_{l} \int_0^{\infty} dr_1 \int_0^{\infty} dr_2 \bar{P}_{ll}^{00}(r_1, r_2) \\ \times P_{ll}^{00}(r_1, r_2, t \to \infty). \end{aligned} \tag{18}$$

The bound radial orbitals, $P_{nl}(r)$, are obtained by diagonalization of the radial Hamiltonian, $T_l(r)$, of equation (7), while the continuum radial orbitals $P_{kl}(r)$, are obtained by solving the radial Schrödinger equation, $\left(T_l(r) - \frac{k^2}{2}\right)P_{kl}(r) = 0$. We note that the projection of the coupled channel radial wavefunctions, $P_{l_1l_2}^{LM}(r_1, r_2, t)$, onto product states after long propagation times has produced very accurate total and differential cross sections in photon, electron, bare ion, and antiproton collisions with a variety of atoms and molecules [16].

The total cross section for single ionization of He is given by

$$\sigma_{+}(n_1l_1, E_n) = 2\sigma_{n\alpha}(E_n) \times \sum_{L} \sum_{l_2} \int_0^{\infty} dk_2 \left| \mathscr{P}_{+}^{L}(n_1l_1, k_2l_2) \right|^2, \tag{19}$$

where the factor of two comes from only projecting onto *nlkl* products and not both *nlkl* and *klnl* products. The total cross section for double ionization of He is given by

$$\sigma_{++}(E_n) = \sigma_{n\alpha}(E_n) \times \sum_{L} \sum_{l_1, l_2} \int_0^{\infty} dk_1 \int_0^{\infty} dk_2 \left| \mathscr{P}_{++}^{L}(k_1l_1, k_2l_2) \right|^2. \tag{20}$$

The energy and angle differential cross section for single ionization of He leaving He^+ in the ground state is given by

$$\frac{d\sigma_{+}(1s, E_n)}{dk\, d\theta\, d\phi} = 2\sigma_{n\alpha}(E_n) \times \left| \sum_{l} (-i)^{l} e^{i\delta_l} \mathscr{P}_{+}^{l}(1s, kl) Y_{l0}(\theta, \phi) \right|^2, \tag{21}$$

where δ_l is the Coulomb phase shift. The energy and angle differential cross section for double ionization of He is given

by

$$\frac{\mathrm{d}\sigma_{++}(E_\mathrm{n})}{\mathrm{d}k_1\mathrm{d}k_2\mathrm{d}\theta_1\mathrm{d}\theta_2\mathrm{d}\phi_1\mathrm{d}\phi_2} = \sigma_{\mathrm{n}\alpha}(E_\mathrm{n}) \times \left| \sum_L \sum_{l_1,l_2} (-\mathrm{i})^{l_1+l_2} \mathrm{e}^{\mathrm{i}(\delta_1+\delta_2)} \mathscr{P}^L_{++}(k_1 l_1, k_2 l_2) \times \sum_{m_1,m_2} C^{l_1 l_2 L}_{m_1 m_2 0} Y_{l_1 m_1}(\theta_1, \phi_1) Y_{l_2 m_2}(\theta_2, \phi_2) \right|^2 . \quad (22)$$

3. Results

For the single and double ionization of He using the TDCC method, we employed a 720 × 720 point radial lattice with a uniform mesh spacing of $\Delta r_1 = \Delta r_2 = 0.20$. For calculations on parallel computers, each 720 point radial mesh was partitioned over 72 core processors. Relaxation of the TDCC equations in imaginary time using the first four coupled channels of table 2 produced a correlated ground state of He. Propagation of the TDCC equations in real time using all 16 coupled channels of table 2 produced total cross sections for single and double ionization of He using equations (19) and (20) for all eight neutron-impact energies of table 1. As a check, we doubled the number of channels in table 2, including up to $L = 4$, and only got a 4% rise in the single photoionization cross section at 200 keV.

A critical factor in obtaining accurate total cross sections was found to be the time length of the propagation of the TDCC equations. With the sudden ejection of the target nucleus following neutron impact, the remaining electrons are found to move rapidly towards the radial box edge. At each time step we multiplied the radial wavefunctions, $P^{L0}_{l_1 l_2}(r_1, r_2, t)$, by a mask function given by

$$M(r_1, r_2) = \left(1 - \mathrm{e}^{-(r_1 - R_1)}\right)\left(1 - \mathrm{e}^{-(r_2 - R_2)}\right), \quad (23)$$

where $R_1 = R_2 = 144.0$. The total probability given by

$$N(t) = \sum_L \sum_{l_1,l_2} \int_0^\infty \mathrm{d}r_1 \int_0^\infty \mathrm{d}r_2 \left| P^{L0}_{l_1 l_2}(r_1, r_2, t) \right|^2 \quad (24)$$

starts off at 1.0 and then decreases as the electrons move toward the box edge. We found that the double ionization cross section, $\sigma_{++}(E_n)$, as a function of time peaks at the same time as $N(t)$ begins to decrease from 1.0. For all eight neutron impact energies of table 1, the peak time is around $t = 30.0$ corresponding to 6000 time steps with $\Delta t = 0.005$ using an explicit 'leapfrog' method [16]. Thus, all of the single and double ionization cross sections are obtained using a total propagation time of $t = 30.0$.

We present total cross sections for the neutron-impact single ionization of He in figure 1. The TDCC results for single ionization leaving He^+ in both ground and excited states is only slightly higher than the TDCC results for single ionization leaving He^+ in only the ground state. Both sets of TDCC results are in reasonable agreement with ECS results [12]. We note that the ECS results are obtained by integrating over the neutron scattering angle the elastic differential cross sections of He.

Table 2. Coupled channels.

Channel	l_1	l_2	L	M
1	0	0	0	0
2	1	1	0	0
3	2	2	0	0
4	3	3	0	0
5	0	1	1	0
6	1	0	1	0
7	1	2	1	0
8	2	1	1	0
9	2	3	1	0
10	3	2	1	0
11	0	2	2	0
12	2	0	2	0
13	1	1	2	0
14	1	3	2	0
15	3	1	2	0
16	2	2	2	0

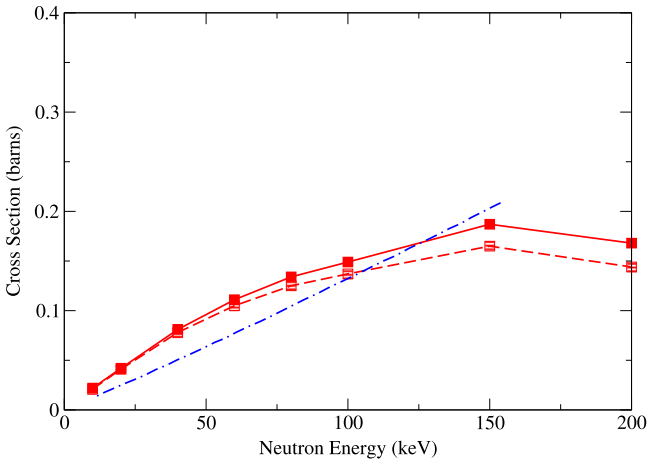

Figure 1. Neutron-impact single ionization of He. Solid line with squares (red): TDCC method for single ionization leaving He^+ in ground and excited states, dashed line with squares (red): TDCC method for single ionization leaving He^+ in ground state, dot-dashed line (blue): ECS method for single ionization [12] (1.0 barn = 1.0 $\times 10^{-24}$ cm^2).

We present total cross sections for the neutron-impact double ionization of He in figure 2. The TDCC results are found to be in reasonable agreement with ECR results [12].

We present double to single total cross section ratios for neutron-impact ionization of He in figure 3. The TDCC results for the ratio of double ionization to single ionization leaving He^+ in both ground and excited states is only slightly lower than the TDCC results for the ratio of double ionization to single ionization leaving He^+ in only the ground state. Both sets of TDCC results are in reasonable agreement with ECR results [12]. We note that both the TDCC and ECR methods predict a rapid rise in the double to single total ionization ratio as a function of neutron-impact energy, in sharp contrast to the gradual decrease in the double to single ratio as a function

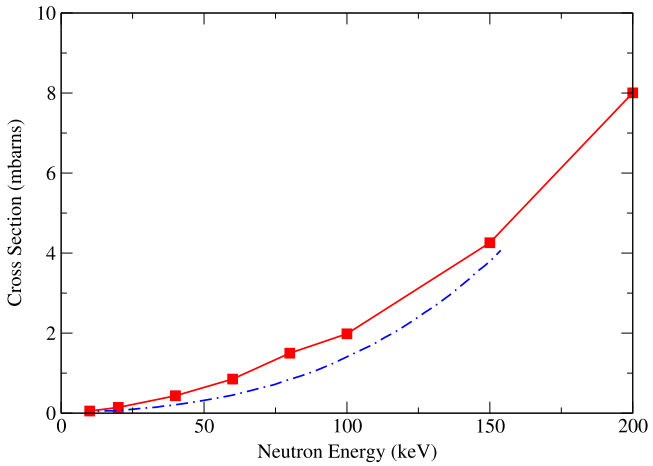

Figure 2. Neutron-impact double ionization of He. Solid line with squares (red): TDCC method for double ionization, dot-dashed line (blue): ECS method for double ionization [12] (1.0 barn = 1.0×10^{-24} cm^2).

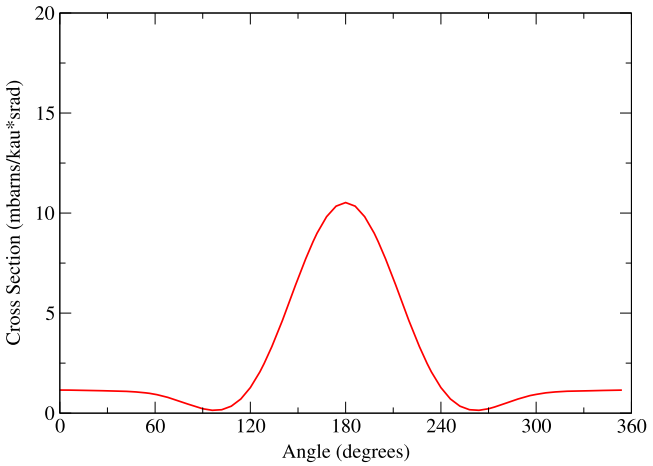

Figure 4. Neutron-impact single ionization of He at 100 keV. Solid line (red): TDCC method for the single ionization differential cross section with $k = 2.0$ and $\phi = 0$ (1.0 mbarn = 1.0×10^{-27} cm^2, kau = momentum in au, srad = solid angle in radians).

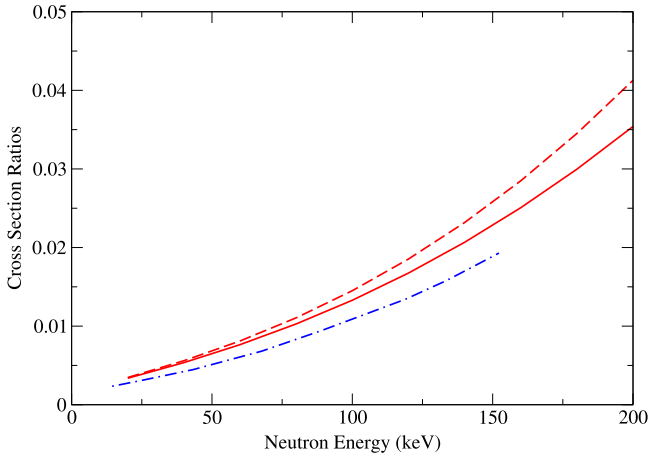

Figure 3. Neutron-impact ionization ratios for He. Solid line (red): TDCC method for the ratio of double ionization to single ionization leaving He^+ in ground and excited states, dashed line (red): TDCC method for the ratio of double ionization to single ionization leaving He^+ in ground state, dot-dashed line (blue): ECS method for the ratio of double ionization to single ionization [12].

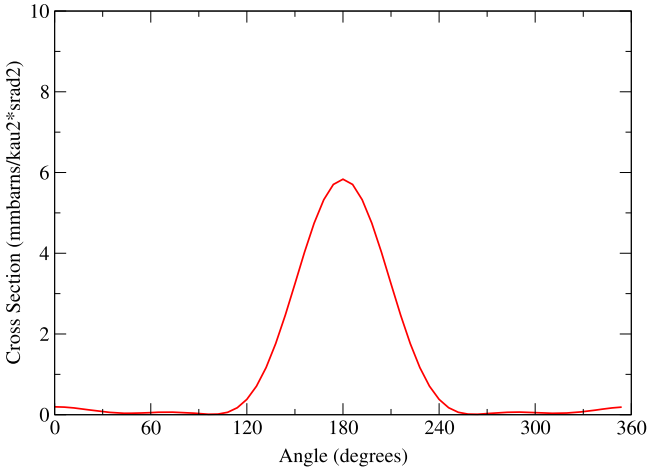

Figure 5. Neutron-impact double ionization of He at 100 keV. Solid line (red): TDCC method for the double ionization differential cross section with $k_1 = k_2 = 2.0$ and $\theta_1 = \phi_1 = \phi_2 = 0$ (1.0 mmbarn = 1.0×10^{-30} cm^2, kau2 = momentum in au squared, srad2 = solid angle in radians squared).

of impact energy seen in charged heavy particle interactions with atoms [17]. At the higher energies the neutron scattering from the nucleus means that the nuclear charge felt by the two electrons is removed very quickly. This enhances double ionization since the electrons will immediately repel each other and rapidly become ionized.

We present energy and angle differential cross sections for the neutron-impact single ionization of He at 100 keV in figure 4. The TDCC results are for single ionization leaving He^+ in the ground state, where the outgoing electron momentum $k = 2.0$ ($E = 54.4$ eV) and $\phi = 0$. We find that the electrons prefer to leave in the opposite direction to the target nucleus.

We present energy and angle differential cross sections for the neutron-impact double ionization of He at 100 keV in figure 5. The TDCC results are for double ionization, where the outgoing electron momenta $k_1 = k_2 = 2.0$ ($E_1 = E_2 = 54.4$ eV) and $\theta_1 = \phi_1 = \phi_2 = 0$. By choosing the first electron to move in the same direction as the target nucleus, the double ionization result should be similar to the single ionization result. The check works out, since we find that the second electron prefers to leave in the opposite direction to the target nucleus.

4. Summary

In this paper we carried out calculations for neutron-impact single ionization, ionization with excitation, and double ionization of He at incident energies between 10 keV and 200 keV using a TDCC method. The cross section prefactor, $\sigma_{n\alpha}(E_n)$, found in equations (19)–(22) made use of NNDC tabulated data for neutron-alpha particle head-on elastic collisions. The key to solving the TDCC equations is a proper formulation of the

initial condition found in equation (14). The TDCC total cross section results for single ionization, double ionization, and the ratio of double to single ionization are found to be in reasonable agreement with ECR results [12]. We also presented TDCC results for energy and angle differential cross sections for both single and double ionization.

In the future, we look forward to experimental confirmation of the neutron-impact double to single ionization cross section ratio at low energy and its rapid rise at high energy as predicted by theory for the He atom. With the experimental development of methods to measure neutron-impact single and double energy and angle differential cross sections for He, we plan to carry out more extensive calculations for a wide variety of ejected electron energies and spatial directions.

Acknowledgments

This work was supported in part by grants from the US Department of Energy and the US National Science Foundation. Computational work was carried out at the National Energy Research Scientific Computing Center in Oakland, California, and the National Center for Computational Sciences in Oak Ridge, Tennessee.

References

[1] Marchalant P J and Bartschat K 1997 *Phys. Rev.* A **56** R1697
[2] Gorczyca T W and Badnell N R 1997 *J. Phys. B: At. Mol. Opt. Phys.* **30** 3897
[3] Selles P, Malegat P and Kazansky A K 2002 *Phys. Rev.* A **65** 032711
[4] Feng L and van der Hart H W 2002 *Phys. Rev.* A **66** 031402
[5] Scott M P, Kinnen A J and McIntyre M W 2012 *Phys. Rev.* A **86** 032707
[6] Kheifets A S and Bray I 1998 *J. Phys. B: At. Mol. Opt. Phys.* **31** L447
[7] Colgan J, Pindzola M S and Robicheaux F 2001 *J. Phys.* B **34** L457
[8] McCurdy C W, Horner D A, Rescigno T N and Martin F 2004 *Phys. Rev.* A **69** 032707
[9] Dorner R *et al* 1998 *Phys. Rev.* A **57** 1074
[10] Berakdar J 2002 *J. Phys.* B **35** L31
[11] Talman J D and Frolov A M 2006 *Phys. Rev.* A **73** 032722
[12] Liertzer M, Feist J, Nagele S and Burgdorfer J 2012 *Phys. Rev. Lett.* **109** 013201
[13] www.ncnr.nist.gov/nsources.html
[14] Collar J I 2013 *Phys. Rev. Lett.* **110** 211101
[15] www.nndc.bnl.gov
[16] Colgan J and Pindzola M S 2012 *Eur. Phys. J.* D **66** 284
[17] Foster M, Colgan J and Pindzola M S 2008 *Phys. Rev. Lett.* **100** 033201